EJN fens EUROPEAN JOURNAL OF NEUROSCIENCE

European Journal of Neuroscience, Vol. 30, pp. 848–859, 2009 doi:10.1111/j.1460-9568.2009.06843.x

BEHAVIORAL NEUROSCIENCE

Fast oscillations in cortical-striatal networks switch frequency following rewarding events and stimulant drugs

J. D. Berke
Department of Psychology and Neuroscience Program, University of Michigan, 530 Church Street, Ann Arbor, MI 48109, USA

Keywords: amphetamine, interneurons, piriform, rats, rhythm, striatum

Abstract

Oscillations may organize communication between components of large-scale brain networks. Although gamma-band oscillations have been repeatedly observed in cortical-basal ganglia circuits, their functional roles are not yet clear. Here I show that, in behaving rats, distinct frequencies of ventral striatal local field potential oscillations show coherence with different cortical inputs. The ~50 Hz gamma oscillations that normally predominate in awake ventral striatum are coherent with piriform cortex, whereas ~80–100 Hz high-gamma oscillations are coherent with frontal cortex. Within striatum, entrainment to gamma rhythms is selective to fast-spiking interneurons, with distinct fast-spiking interneuron populations entrained to different gamma frequencies. Administration of the psychomotor stimulant amphetamine or the dopamine agonist apomorphine causes a prolonged decrease in ~50 Hz power and increase in ~80–100 Hz power. The same frequency switch is observed for shorter epochs spontaneously in awake, undrugged animals and is consistently provoked for < 1 s following reward receipt. Individual striatal neurons can participate in these brief high-gamma bursts with, or without, substantial changes in firing rate. Switching between discrete oscillatory states may allow different modes of information processing during decision-making and reinforcement-based learning, and may also be an important systems-level process by which stimulant drugs affect cognition and behavior.

Introduction

Cortical-basal ganglia loop circuits have a vital role in normal learning and decision-making, and dysfunction of these circuits is implicated in a wide range of human neurological and psychiatric disorders. Although classic 'box-and-arrow' models of basal ganglia organization (Albin *et al.*, 1989; Mink, 1996) have spurred much fruitful research, it has also been recognized for some time that we require greater knowledge about the dynamics of brain activity in these circuits to reveal their operational principles. Along these lines there has been recent interest in oscillations and synchrony within the basal ganglia, in both normal and pathological states (Bevan *et al.*, 2002; Hammond *et al.*, 2007). In particular, there is evidence that dopamine depletion in Parkinson's disease leads to enhanced beta frequency (~20 Hz) synchronization in the basal ganglia (Cassidy *et al.*, 2002) that can be reversed with therapeutic treatments including dopaminergic drugs and deep brain stimulation (Kuhn *et al.*, 2008). However, the normal functional role(s) of oscillations in these circuits is poorly understood, in part because they have most commonly been investigated in anesthetized and/or restrained animals (e.g. Ruskin *et al.*, 1999; Magill *et al.*, 2000; Tseng *et al.*, 2001) rather than during active task performance.

Correspondence: Dr J. D. Berke, as above.
E-mail: jdberke@umich.edu

Received 26 April 2009, revised 4 June 2009, accepted 11 June 2009

In the striatum of freely moving rats, prominent local field potential (LFP) oscillations occur in several frequency bands including theta (~8 Hz), beta (~20 Hz) and gamma (35–100 Hz; Berke *et al.*, 2004). The striatal theta rhythm is coherent with hippocampus, indicating that the striatum is one of a set of brain regions, also including amygdala and medial frontal cortex, that share a common theta modulation (Pare & Gaudreau, 1996; Buzsáki, 2002; Jones & Wilson, 2005). Theta coherence between these structures may serve to facilitate information exchange, for example during memory storage and manipulation.

Faster rhythms such as gamma oscillations are thought to help to organize ensembles of synchronously firing neurons in various brain regions, including olfactory structures (Laurent, 2002; Kay *et al.*, 2009) and hippocampus (Harris *et al.*, 2003), and may play a key role in top-down mechanisms controlling cortical processing, such as attention (Fries *et al.*, 2001). Fast LFP rhythms have also been previously reported in the human basal ganglia, including subthalamic nucleus (Fogelson *et al.*, 2005) and most recently striatum (Cohen *et al.*, 2009). However, the great majority of individual rat striatal neurons do not show obvious entrainment to local beta or gamma rhythms (Berke *et al.*, 2004) and it is not clear how these striatal rhythms relate to oscillations elsewhere.

To increase understanding of striatal fast rhythms, I examined whether they match oscillations occurring in nearby and interconnected structures, and compared the participation of distinct

striatal cell types. Further, I assessed how these oscillations change during behavioral task performance and in response to dopaminergic manipulations known to affect behavior via actions in striatum.

Materials and methods

The data set used here is the same as in Berke *et al.* (2008) and Berke *et al.* (2009), and experimental procedures have been previously described in detail. All procedures were in accordance with US National Institutes of Health guidelines, and were approved by the Boston University and University of Michigan Institutional Animal Care and Use Committees. Thirsty adult male Long-Evans rats ran between water ports at the ends of the arms of a four-arm radial maze, guided by flashing cue lights at the entrances to maze arms. Frame-by-frame video analysis and running speed measurements were used to determine the moments at which rats began to accelerate down the selected maze arm ('choice') and when their nose reached the reward ports. When radial maze experiments were completed, some animals were placed on a familiar holding stool and, following collection of baseline data, injected with either isotonic saline, apomorphine or D-amphetamine sulfate dissolved in saline. Drugs were obtained from Sigma–Aldrich Inc. The main focus of these experiments was the striatum and dorsal hippocampus (CA1) but some animals also had histologically-verified tetrode placements in medial frontal cortex ($n = 2$) and piriform cortex ($n = 3$). In addition, electrocorticogram (ECoG) signals were routinely recorded from skull screws placed over frontal cortex (AP, 4.5–5.0; ML, 1.0–2.5 mm relative to bregma) and olfactory bulb (AP, 6.7–7.0; ML, 1.0), in all cases ipsilateral to tetrodes. All simultaneously recorded LFP and ECoG signals were referenced to the same location (another skull screw, typically placed at 1.0 mm posterior to lambda) and digitized at 1024 or 1500 samples/s.

Analyses were performed in MATLAB (Mathworks Inc.) and/or Neuroexplorer (Nex Technologies). Session-wide power spectra were calculated using Welch's method (1024 frequencies between 1 and 200 Hz, smoothed with a Gaussian kernel with half-width of 3 points). Coherence analysis, which measures whether oscillations in two sites show a consistent phase relationship (Nunez & Srinivasan, 2006), was performed with the same parameters except that 512 frequencies were used. To assess the effects of drug injections on LFP power, 10 min blocks of time before and after injection were compared. To obtain a baseline period with a normal, alert waking state, care was taken to avoid extended periods of time in which the ECoG and LFP signals showed large-amplitude, low-frequency activity indicative of slow-wave sleep; inspection of spectrograms in all animals led to the selection of the −12 to −2 min epoch. The post-drug epoch used to assess amphetamine effects was 1 h post-drug (+ 55 to + 65 min), as this was a period of approximately maximal drug effect on behavior; results were not sensitive to the particular epoch used. Apomorphine has a shorter duration of action and so an earlier epoch (+ 5 to + 15 min) was used as the post-drug period. For transient behavior-linked power changes, the spectra in 1 s LFP windows were calculated using the multi-taper routine '`pmtm`' (with 1 Hz resolution and four tapers). Multi-taper spectrograms were calculated using the '`mtspecgramc`' routine from the Chronux library, with a 3 s window sliding in 1 s intervals, on LFPs downsampled from 1024 to 256 samples/s. To visualize fast changes in LFP power surrounding behavioral events, averaged, triggered wavelet scalograms (Addison, 2002) were constructed by convolving the LFP signal (downsampled to 512 samples/s) with a complex Morlet wavelet (with angular frequency $w_0 = 25$ and 120 scales corresponding to a 1 Hz resolution between 1 and 120 Hz). Very similar results were obtained using spectrograms with brief time windows but the wavelets are shown here because they gave a superior combination of time and frequency resolution.

Spike waveforms are shown with negative polarity up and with standard distortion produced by hardware filtering at 300–6000 Hz (Wiltschko *et al.*, 2008). Although individual neurons were often recorded across multiple daily sessions, I wished to avoid repeated analysis of the same cells as this could produce a misleading picture of neuronal populations. To this end, neurons from a given probe were only analysed once, unless the probe had been moved at least ∼100 μm between sessions. Only neurons that fired a minimum of 100 spikes were included in analyses.

I tested for oscillatory entrainment using a multiple-step procedure. First I examined the spike-triggered average (STA) LFP, over the whole session of task performance, to identify promising candidate neurons. For each neuron the STA was calculated as the mean of the raw LFP segments in a [−0.125 0.125]s window surrounding each spike, across the whole session. Qualitatively, 'strong' oscillatory entrainment was taken as a rhythm in the STA, centered near zero (i.e. spike times) and tapering towards the window edges, whose peak–trough magnitude was $> 2 \times$ SEM. I then calculated the spike-field coherence (SFC) spectrum (e.g. Fries *et al.*, 2001) to determine specific potential frequency ranges of entrainment. The SFC was calculated as the power spectrum of the STA divided by the mean of the power spectra of the individual LFP segments surrounding each spike. The SFC helps to normalize for the power of rhythmic activity that is present in the LFP but without a relationship to spike times. Note that SFC values will tend to be lower as frequency increases, as high-frequency rhythms will generally appear in only a small central portion of the STA window used. Finally I produced phase histograms showing the extent and significance of entrainment to the LFP filtered in those frequency ranges (Fig. 2). Significance of entrainment was assessed by calculating a Rayleigh's Z score for the resulting circular distribution, as previously described (Berke *et al.*, 2004; Berke *et al.*, 2008). Determining spike–LFP relationships when both signals are recorded from the same probe can give misleading results due to incomplete removal of spikes from the LFP signal (Berke, 2005). To avoid this, all striatal spike–LFP relationships were reassessed using LFPs from a nearby probe, yielding very similar or identical results.

Results

Oscillations in striatal LFPs show frequency-dependent coherence with other brain regions

Gamma rhythms are known to be very prominent in olfaction-related structures such as olfactory bulb and piriform cortex (Kay *et al.*, 2009) and, like other cortical regions, piriform cortex has unidirectional projections to striatum (Neville & Haberly, 2004). I therefore assessed whether the ∼50 Hz striatal gamma oscillations are the same as, or quite distinct from, piriform cortex oscillations. The example shown in Fig. 1 is one of three animals for which tetrode recordings were obtained simultaneously in ventral striatum and piriform cortex; in every case piriform cortex showed ∼50 Hz oscillations that appeared identical to the striatal ∼50 Hz rhythm, with coherence close to unity. The striatal ∼50 Hz rhythm consistently resembled a lower-power version of piriform ∼50 Hz oscillations and became weaker with increasing distance from piriform cortex (as in Fig. 1). The ∼50 Hz oscillations were consistently stronger in piriform cortex and ventral striatum than in other structures that were recorded from, including dorsal hippocampus (CA1) and medial frontal cortex (Fig. 1), although a ∼50 Hz peak in coherence between all structures was commonly seen. I conclude that the ∼50 Hz oscillations recorded in

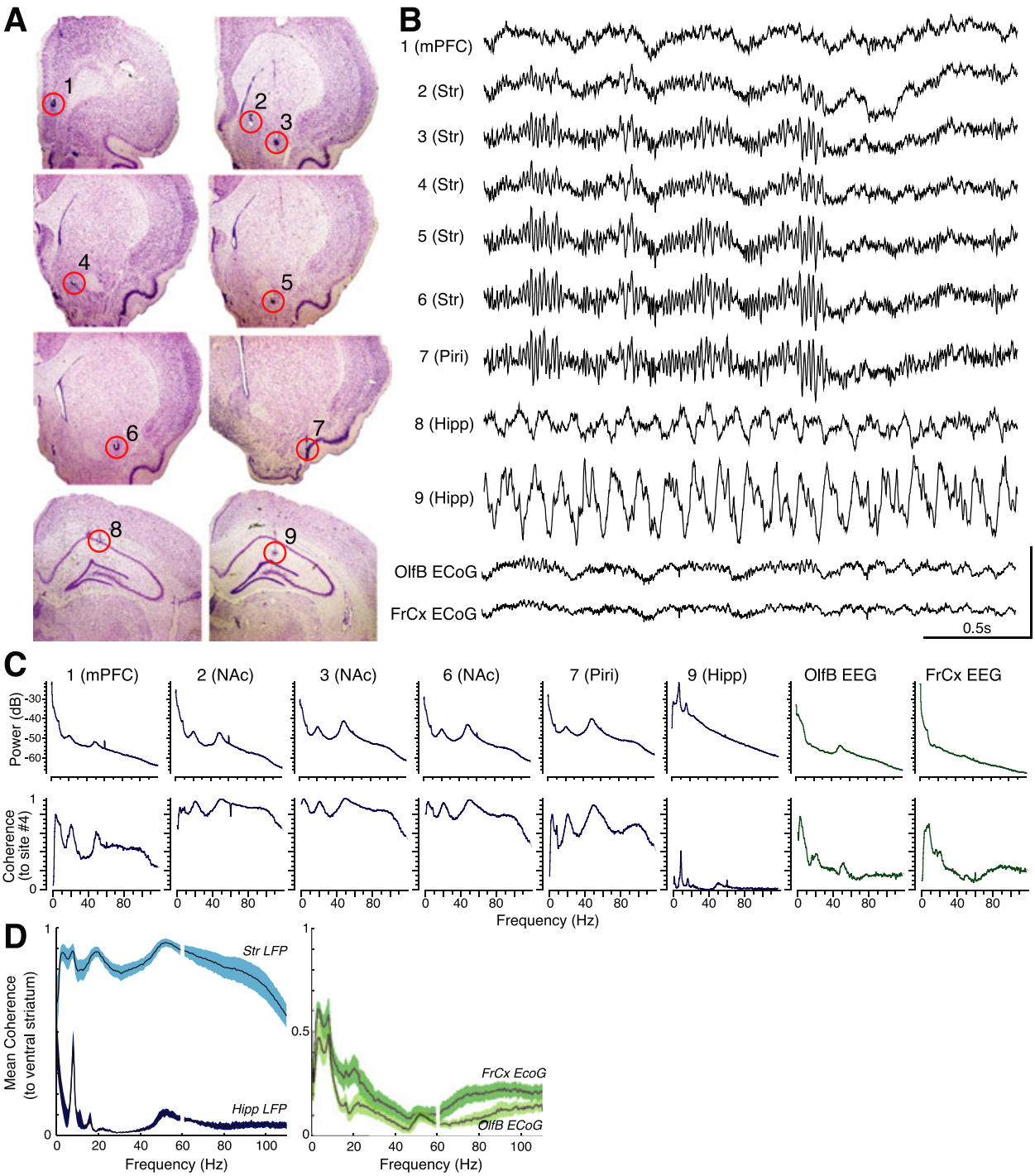

FIG. 1. Comparison of oscillations in awake ventral striatum and other interconnected regions. (A) Coronal rat brain sections showing an example of simultaneous tetrode placements in medial frontal cortex (mPFC; 1), ventral striatum (Str; 2–6), piriform cortex (Piri; 7) and dorsal hippocampus (Hipp; 8 and 9). (B) LFPs recorded from the locations shown in A during performance of a radial maze task. Also shown are ECoG recordings from skull screws placed over ipsilateral olfactory bulb (OlfB; AP, 7; ML, 1 mm relative to bregma) and frontal cortex (FrCx; AP, 5; ML, 2.5 mm). All signals are referenced to the same location (see Materials and methods). Note theta (~8 Hz) rhythm that is most prominent in deep hippocampal layers (9) and large-amplitude high-frequency oscillation (~50 Hz) that is most prominent in piriform cortex and nearby regions of ventral striatum, and also visible to a lesser degree in olfactory bulb ECoG. (C) Power spectral density (top) and coherence (bottom) plots for a subset of the recording sites illustrated in A and B. In all cases coherence was calculated to LFP at site 4. Coherence is high for all frequencies when comparing sites within ventral striatum but resolves into more discrete frequency bands when comparing ventral striatum with other structures. (D) Mean coherence spectra between ventral striatal LFP and another site in ventral or central striatum (left, light blue), dorsal hippocampus CA1 pyramidal layer (left, dark blue), frontal cortex ECoG (right, dark green) and olfactory bulb ECoG (right, light green) (n = 7, all rats for which all of these signals were simultaneously recorded). Each plot shows mean ± SEM (shaded area). Points immediately surrounding 60 Hz are omitted due to occasional contributions of line noise. Coherence is high for all frequencies between two striatal sites but is selective to theta oscillations between striatum and hippocampal CA1. Coherence in the high-gamma range is consistently higher between striatum and frontal cortex ECoG than between striatum and olfactory bulb ECoG or between striatum and posterior cortex ECoG (not shown).

striatum are another manifestation of classical gamma rhythms that were discovered in the olfactory system (Adrian, 1942; Rojas-Libano & Kay, 2008) but which also percolate into a variety of forebrain structures.

In addition to the prominent ~50 Hz peak, striatal LFP power spectra typically show a weaker, broader hump in the high gamma range (~80–100 Hz; Fig. 1C). This high-gamma activity was also apparent in the coherence spectra, both within ventral striatum and between striatum and some other structures, including piriform and frontal cortex. Although most animals did not have simultaneous tetrode placements in all investigated brain regions, for seven rats I did have simultaneous striatal and hippocampal tetrode LFP recordings, together with ECoG recordings from skull screws above both frontal cortex and olfactory bulb. Between striatum and hippocampal CA1 coherence was high only for the theta rhythm; high-gamma coherence was never observed (e.g. Fig. 1C). However, high-gamma coherence was consistently and selectively found between frontal cortex and striatum (Fig. 1C and D). For all seven animals, frontal cortex/striatum coherence was higher at 80 than 50 Hz (binomial test, $P < 0.01$). In addition, 80 Hz coherence was always higher between these structures than between olfactory bulb and striatum (binomial test, $P < 0.01$). Oscillations in the awake striatal LFP thus appear to reflect participation in at least three overlapping brain networks: a theta network that includes hippocampus, a ~50 Hz network that includes piriform cortex and olfactory bulb, and a ~80–100 Hz network that includes frontal cortex.

Selective entrainment of striatal fast-spiking interneurons to specific gamma-frequency oscillations

The LFP signals recorded in a given location can arise either from physiological processes at that location or by volume conduction from other brain regions. It is therefore important to demonstrate that individual neurons are entrained to these rhythms, in order to gain confidence that they actually reflect local physiological activity.

Although I recorded from only a small number of piriform cortex cells, a high proportion of them [7/8 cells (87.5%) from two rats] showed very strong entrainment to ~50 Hz (e.g. Fig. 2, Ai), consistent with previous studies of piriform cell entrainment (e.g. Eeckman & Freeman, 1990). By contrast, comparably strong cell entrainment to any oscillation faster than theta was rare in the striatum [8/182 cells (4.4%) from 13 rats; e.g. Fig. 2, Aii, Aiii and B]. In particular, among the presumed medium spiny projection neurons (MSNs) that make up 90–95% of striatal neurons, none showed strong beta or gamma entrainment across the whole behavioral session (0/122 cells), although a weak gamma-band modulation was sometimes observed (Fig. 2, Aiv).

Strikingly, however, all of the strongly entrained striatal cells showed characteristics of presumed GABAergic interneurons, such as high firing rates, brief waveforms and capacity to fire spikes at very short interspike intervals. Six of the eight strongly entrained cells (from five different rats) met all of the previously established criteria for presumed parvalbumin-positive, fast-spiking interneurons (FSIs) (Berke *et al.*, 2004; Mallet *et al.*, 2005; Berke, 2008) [6/37 FSIs (16.2%) were strongly entrained]. FSIs are rare (~1% of striatal neurons; Luk & Sadikot, 2001) GABAergic cells that are thought to have a critical role in the control of MSN spike timing, via $GABA_A$ signaling at perisomatic synapses (Koos & Tepper, 1999; Koos *et al.*, 2004), and in other forebrain circuits FSIs have a critical role in the pacing and control of gamma oscillations (Buzsáki, 2006; Fries *et al.*, 2007).

When strong FSI entrainment was observed, it was apparent in STAs of LFPs recorded throughout striatum, including sites very distant from the probe from which the spikes were recorded (Fig. 2B). However, individual FSIs did not participate in all rhythms but select subsets. For example, of the two striatal FSIs shown in Fig. 2, Aii and Aiii, the first fired spikes entrained to beta and ~50 Hz, whereas the second was entrained to theta and ~80 Hz. Although FSIs form an electrically-coupled meshwork within striatum (e.g. Fukuda, 2009), I also observed that, even within a very small region of striatum, distinct FSIs could show very distinct patterns of entrainment. For example, the cell in Fig. 2B was recorded simultaneously, on the same probe, with another FSI that lacked clear oscillations in the STA (not shown).

Dopaminergic drugs cause a switch in the frequency of striatal gamma oscillations

Drugs that alter dopamine neurotransmission in cortical-striatal circuits can have powerful effects on arousal, motivation and learning. I therefore investigated how dopaminergic drugs affect fast oscillations within the awake striatum.

Both the psychomotor stimulant amphetamine, which enhances striatal dopamine release, and the direct mixed D_1/D_2 receptor agonist apomorphine caused a profound shift in striatal LFP frequencies (Fig. 3). Most obviously, the prominent ~50 Hz band was abolished and replaced by a broad range of higher frequency gamma rhythms (~70–100 Hz). The duration of this switch in gamma frequencies paralleled the time course of drug-induced behavioral activation (locomotor activity and stereotyped sniffing; not shown). A prolonged gamma switch did not occur in animals given saline injections (Fig. 3), although in some cases such injections produced bouts of high-gamma oscillations lasting just a minute or two. In addition, spontaneous shorter transitions to high-gamma oscillations were often observed (e.g. see pre-drug periods in Fig. 3). This suggests that the high-gamma oscillations are one of a set of normal, yet mutually exclusive, states of cortical-striatal circuitry, rather than an abnormal condition produced by drugs.

Piriform cortex and olfactory bulb have been previously shown to switch between ~50 Hz ('gamma2') and ~70 Hz ('gamma1') rhythms (Rojas-Libano & Kay, 2008; Kay *et al.*, 2009). Although the specific functions of these rhythms are not understood, ~70 Hz rhythms seem to occur more during active sniffing (Kay, 2003). Might a drug-induced change in sniffing behavior, reflected in altered olfactory rhythms, account for the change in striatal gamma frequencies seen here? To investigate this I examined power and coherence patterns in two of the amphetamine-treated animals, for which I had frontal cortex and olfactory bulb ECoG recordings as well as striatum (Supporting information, Fig. S1). Amphetamine increased high-gamma power in both frontal cortex and olfactory bulb; however, evoked high gamma had a different frequency composition in these two sites, tending towards ~70 Hz in olfactory bulb and 80–100 Hz in frontal cortex. Within the gamma band, post-amphetamine coherence between striatum and olfactory bulb was highest at ~70 Hz, whereas coherence between striatum and frontal cortex was highest at 80–100 Hz. These results suggest that drug-evoked high-gamma oscillations in striatum are a combination of (at least) two distinct processes, i.e. the previously described ~70 Hz olfaction-related rhythm and increased power in the ~80–100 Hz network that includes frontal cortex.

Transient gamma-frequency switching during behavioral task performance

As the frequency of fast oscillations can show spontaneous switching even without drug manipulations, I next examined whether this

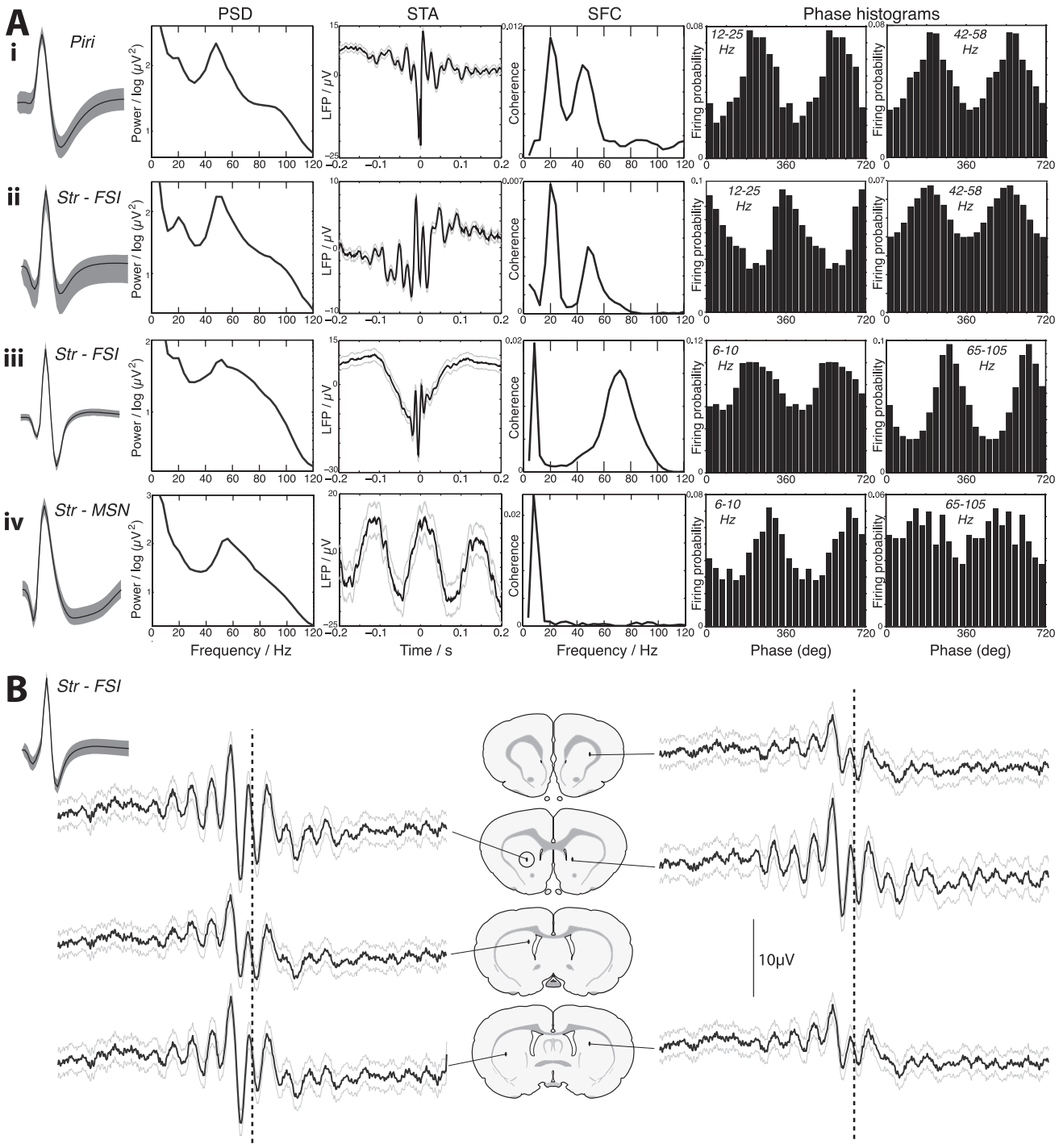

FIG 2. Entrainment of neurons to LFP oscillations. (A) Analysis of four individual neurons (rows i–iv) recorded during maze task performance. From left to right, filtered spike waveform (mean ± SD), mean power spectral density (PSD) of 0.25 s LFP segments surrounding each spike, STA (± 2 × SEM), SFC and phase histograms for selected frequency bands (see Materials and methods). Neurons i and ii were recorded from locations 7 (piriform cortex) and 5 (striatum) in Fig. 1, respectively; other neurons are from separate animals. Significance of spike entrainment to LFP oscillations was assessed from the phase histograms, with results as follows. Neuron i (piriform, total spike count = 37 843 during 2532 s), 2823 LFP beta troughs identified from 147.1 s of detected high 12-25 Hz power, beta-entrained with mean spike vector size $r = 0.283$, phase $\varphi = -125.0°$, significance $P = 2.18 \times 10^{-24}$; 11 577 ~ 50 Hz troughs identified from 222 s of detected high 42–58 Hz power, ~50 Hz entrained with $r = 0.221$, $\varphi = -151.7°$, $P = 5.72 \times 10^{-71}$. Neuron ii (striatal FSI, total spike count = 99 419 over 2748 s), 2001 LFP beta troughs identified from 97.7 s of detected high 12–25 Hz power, beta-entrained with $r = 0.231$, $\varphi = 18.9°$, $P = 2.99 \times 10^{-52}$; 29 160 ~50 Hz troughs identified from 575 s of detected high 42–58 Hz power, ~50 Hz entrained with $r = 0.135$, $P = 8.47 \times 10^{-139}$. Neuron iii (striatal FSI, total spike count = 82 014 over 2437 s), 23 968 ~80 Hz troughs identified from 301.5 s of high 65–105 Hz power, ~80 Hz entrained with $r = 0.327$, $\varphi = -73°$, $P < 2.23 \times 10^{-308}$. Neuron iv (striatal MSN, total spike count = 7316 over 2753 s), 13 306 ~80 Hz troughs identified from 172.0 s of high 65–105 Hz power, ~80 Hz entrained with $r = 0.101$, $\varphi = 161°$, $P = 0.03$ (but n.s. if multiple comparisons are considered). (B) Another example of a ~50 Hz-entrained striatal FSI, recorded from the circled site, showing STAs (44 275 spikes over 1495 s; −0.2 to + 0.2 s analysis range, as in A) of LFPs recorded simultaneously from each of the indicated locations. ~50 Hz entrainment is clear even for LFPs from distant and contralateral striatal locations. Dotted line indicates spike times. Note that all LFP traces are in phase despite widely separated locations.

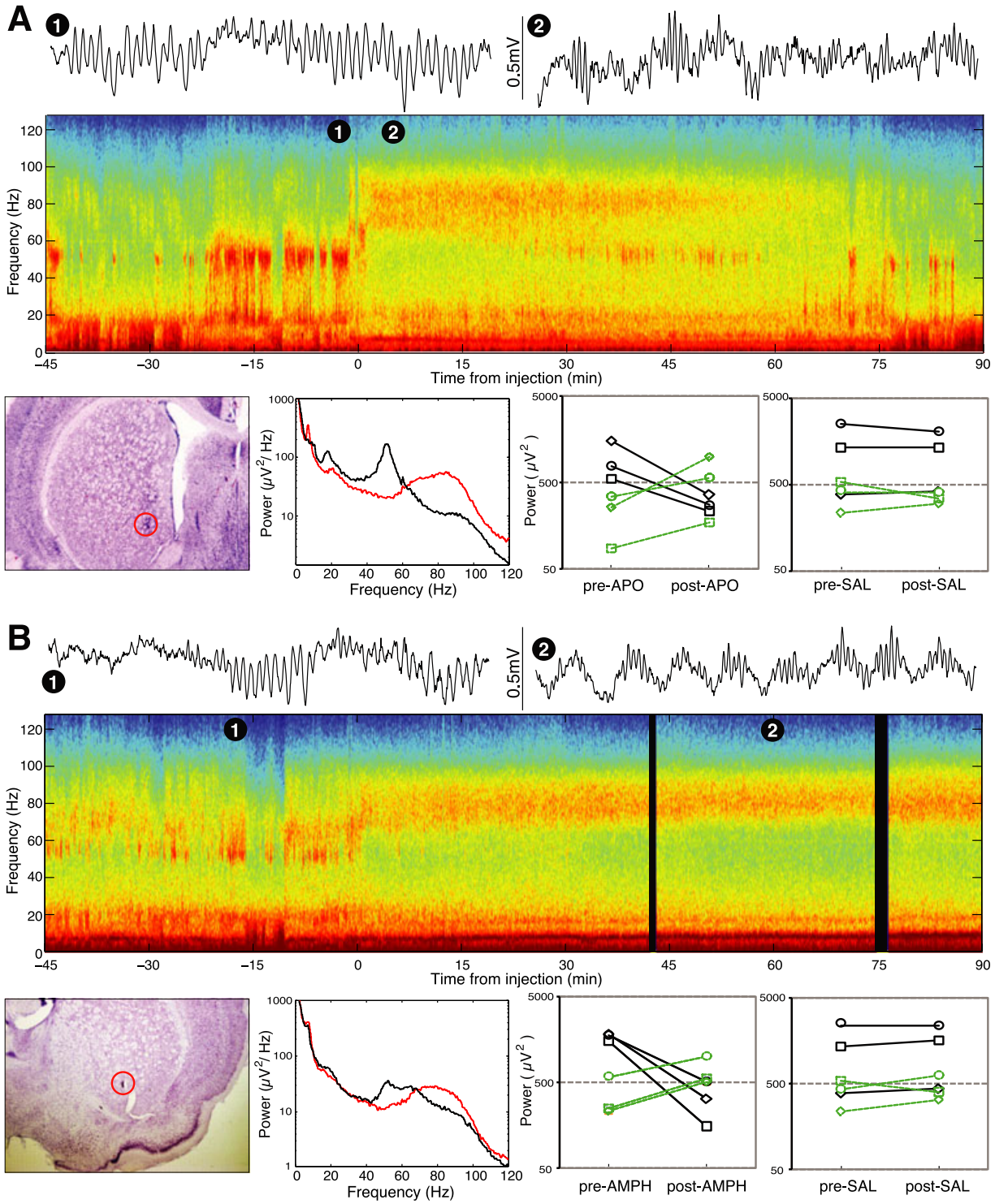

FIG. 3. Effects of systemic drug administration on striatal LFP oscillations. (A) Effects of the direct dopamine agonist apomorphine (2 mg/kg, i.p.). Top, striatal LFP traces (1 s duration each) pre- (left) and post- (right) drug injection. Middle colored panel shows a spectrogram of LFP power, with drug injection at time 0. 1 and 2 indicate times from which the LFP traces were taken. Lower left panel shows coronal brain section with striatal tetrode recording site marked. Adjacent lower panel shows LFP power spectral density comparing before (black, −12 to −2 min relative to injection) with after (red, + 5 to + 15 min). Lower right panels show power in the 42–58 Hz (black) and 70–90 Hz (green) bands for rats (distinct symbols) given apomorphine (APO) (left) and the same animals given saline (SAL) (right). Time epochs used are the same as in the power spectral density. All animals showed a clear decrease in ∼50 Hz gamma power and an increase in ∼80 Hz gamma power in response to apomorphine but not saline injection. (B) Effects of the indirect dopamine agonist amphetamine (AMPH; 2.5 mg/kg, i.p.). Layout is the same as for A, except that the 'post-drug' period used for power analysis was 1 h after drug injection (55–65 min). Effects are similar to apomorphine but longer-lasting (in parallel with the more extended behavioral effects of this drug). Note the theta-nested gamma oscillations in the raw LFP trace post-amphetamine. Black regions in the spectrogram indicate time epochs during which recording was suspended. Epochs in the pre-drug period without gamma oscillations correspond to sleep, in which ∼50 Hz oscillations are absent (Berke *et al.*, 2004).

phenomenon was reliably associated with specific aspects of behavior during a radial maze task (Berke *et al.*, 2009). I constructed averaged, event-triggered wavelet scalograms, aligned on either the onset of the instruction cue, the moment at which the rat began to accelerate towards the chosen goal, or the moment at which the rat's nose reached the baited or unbaited reward port. I found that arrivals at the reward ports were associated with a dramatic, transient decrease in ~50 Hz power and an increase in high-gamma power (Fig. 4). Once again, evoked high-gamma power occupied a broad frequency range that may reflect multiple oscillatory processes. Nonetheless, striatal coherence with frontal cortex ECoG was maintained or even increased [mean 70–90 Hz coherence: 0.193 during (−1.5 to −0.5 s) epochs before rewards; 0.241 during (0.5 to 1.5 s) epochs after, $n = 7$ rats], whereas high-gamma coherence with both olfactory bulb ECoG and hippocampal CA1 LFP remained low.

To assess whether this switch in gamma rhythms was specific to actually receiving rewards, I examined behavioral sessions in which the rats were still learning the radial maze task and thus made similar numbers of correct and incorrect responses ($n = 7$ rats, one session each; mean number of rewarded trials = 77.8, range 52–97; mean number of unrewarded trials = 55.4, range 36–70). All animals showed a significant reduction in 42-58 Hz power, and a significant increase in 70–90 Hz power, for both rewarded and unrewarded trials (comparing the interval −1.5 to −0.5 s with 1.5 to 0.5 s relative to water port arrival; Wilcoxon signed rank test, $P < 10^{-7}$ for every comparison). However, for six of seven animals the transient pulse of

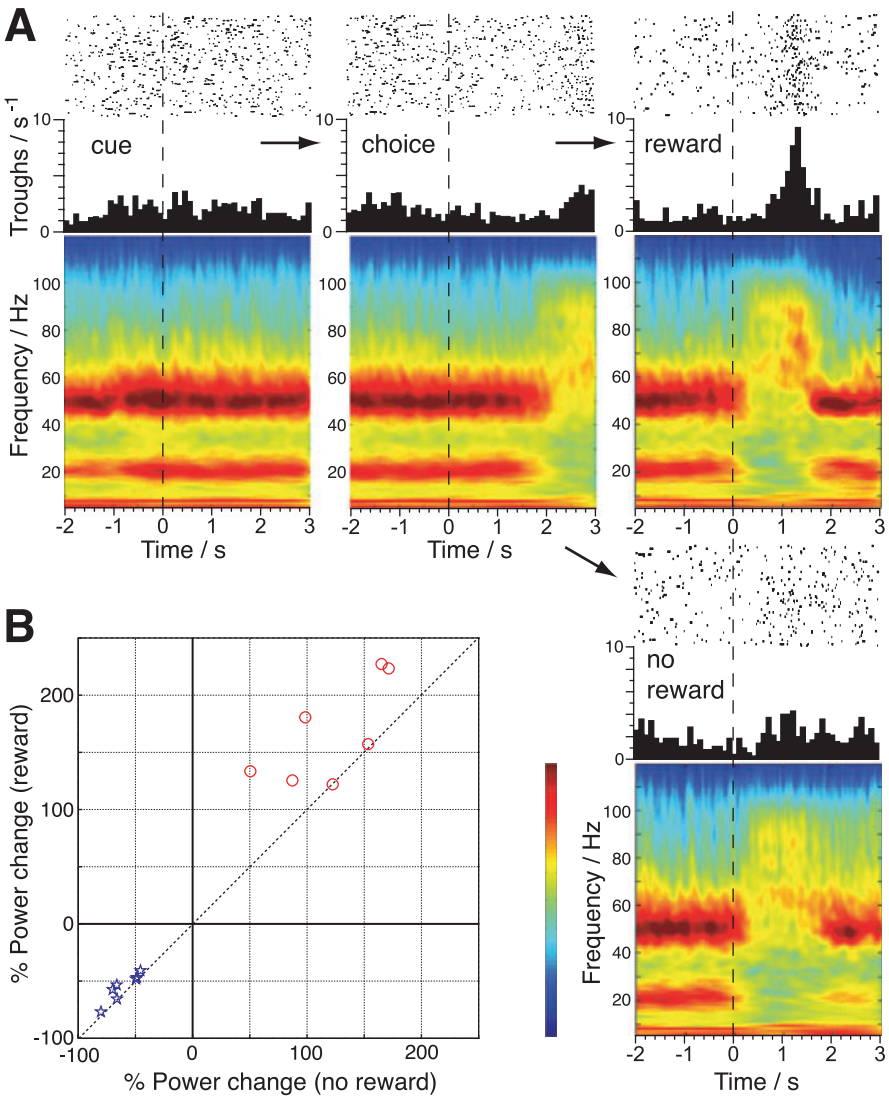

FIG. 4. Transient gamma frequency switching following reward delivery in a radial maze task. (A) Power changes associated with specific events in a radial maze task. Upper panels show rasters and histograms of detected troughs of high-gamma oscillations, within epochs of high power in the 65–105 Hz filtered signal. LFP used was from ventral striatal site 5 in Fig. 1 (very similar or identical results were also obtained from other ventral striatal sites in the same animal). Analyses are aligned on 'cue' (onsets of flashing instruction cues; $n = 162$), 'choice' (times at which rat began to accelerate down chosen arms; $n = 162$), 'reward' (arrivals at baited reward port; $n = 92$) or 'no reward' (arrivals at unbaited ports; $n = 70$). Histograms use 100 ms bins without smoothing. Lower colored panels are the corresponding averaged triggered wavelet scalograms (all using the same color scale). Note that arrival at reward ports is associated with an interruption in ~50 Hz (and beta) power and a transient burst of high ~80 Hz power. The ~80 Hz burst was more powerful on correct trials than incorrect trials (mean 70–90 Hz power in + 0.5 to + 1.5 s epoch, 52.5 vs. 41.4 $\mu V^2/Hz$, Mann–Whitney–Wilcoxon test $z = -4.67$, $P = 3.0 \times 10^{-6}$). (B) Gamma power changes for all analysed animals ($n = 7$). Red circles show change in 70–90 Hz power, blue stars show change in 42–58 Hz power, again comparing the epochs (−1.5 to −0.5 s) to (+ 0.5 to + 1.5 s) relative to arrivals at reward ports. All animals showed large increases in ~80 Hz power and decreases in ~50 Hz power.

70–90 Hz power was significantly stronger in rewarded than unrewarded trials (Mann–Whitney–Wilcoxon rank test, $P < 0.005$ for each of those six rats, $P = 0.325$ for the other rat). No marked frequency shifts were apparent in conjunction with other salient task events, although this maze task is not optimized for precisely determining, the moments at which decisions are made.

Single striatal neurons can participate in transient high-gamma oscillations

Finally, I explored how these switches in gamma oscillations may affect striatal information processing, by looking for changes in the firing of gamma-entrained striatal neurons following reward detection in the maze task. I have previously reported that FSIs show idiosyncratic behavior-linked firing rate changes in this task (Berke, 2008) and no consistent rate change was seen among gamma-entrained cells during the brief epoch of increased high-gamma oscillations. However, I did observe two clear examples in which spike timing indicated neuronal participation in the transient high-gamma epoch (Fig. 5). One case (Fig. 5, left) was an FSI that normally showed strong ∼80 Hz entrainment (same cell as Fig. 2, Aiii); this cell showed no clear firing rate change during rewards but a transient increase in ∼80 Hz SFC following rewards (Fig. 5D). As SFC is theoretically normalized for LFP power, this suggests that this cell is becoming even more precisely phase-locked to local ∼80 Hz oscillations during this epoch, although a more conservative interpretation is simply that this cell continues to participate in high-gamma rhythms as these oscillations become transiently stronger. Another case (Fig. 5, right) involved a cell that was not easily classified due to a complex spike waveform but that like FSIs was capable of firing spikes at very short intervals (Fig. 5C). This cell was normally phase-locked to ∼50 Hz striatal oscillations but, following arrival at the reward ports, the cell transiently showed both an increase in firing rate and a marked switch to high-gamma entrainment. Although further conclusions about the behavior of subpopulations of striatal neurons during high-gamma epochs would require a larger database of entrained cells, these examples show that individual striatal cells can participate in transient gamma frequency shifts and can do so with, or without, firing rate changes.

Discussion

To better understand the significance of gamma oscillations in striatal LFPs, I adopted a combined 'macrocircuit/microcircuit' approach, investigating both relationships to activity in other, interconnected brain regions and the participation of specific neuron types. Consistent with the convergent projections to ventral striatum, I found that oscillations there may largely be a superposition of distinct oscillations found in afferent limbic circuitry. The piriform cortex and striatum share strong common rhythmic activity, particularly at ∼50 Hz, whereas the frontal cortex is more involved in higher frequency (≥ 80 Hz) oscillations. Cortical-striatal networks appeared to switch between these rhythms, both spontaneously and during the detection of natural rewards, and prolonged high-gamma oscillations could be produced by dopaminergic drugs. Strong striatal cell entrainment to gamma oscillations was rare, but clearly present and selective to FSIs, and these cells could participate in epochs of enhanced high-gamma power even without overt firing rate changes. Overall, these findings clearly demonstrate a correlation between behavioral states and fast oscillations in cortical-striatal circuits. At the same time, several critical questions about these oscillations remain unanswered and will be important topics for future investigation.

What are striatal gamma oscillations and where do they come from?

The piriform cortex possesses an orderly arrangement of neuronal elements in layers, and the sequence of synaptic events producing LFP gamma oscillations there is relatively well characterized (e.g. Neville & Haberly, 2004). In contrast, the mechanisms of LFP generation in non-laminar structures such as striatum are very poorly understood (Berke, 2005), as spatially separated current sources and sinks cannot be readily identified. Given the very large 50 Hz gamma generated by piriform, and the apparently steady decrease in striatal 50 Hz power with distance from piriform (Fig. 1), it is quite likely that a significant part of the striatal 50 Hz signal reflects volume conduction. At the same time, the fact that a substantial number of FSIs were very strongly entrained to fast rhythms conclusively demonstrates that these rhythms are not *just* volume conducted from adjoining structures such as piriform cortex. A likely similar situation involves the theta rhythm recorded in the parietal cortex overlying hippocampus. There many cortical cells show modulation relative to intracortical theta rhythms that may be functionally significant, even though this theta is largely volume conducted from hippocampus (Sirota *et al.*, 2008). Overall, the most reasonable estimate possible from the data presented here is that striatal LFP fast oscillations reflect a broad combination of volume conduction from other structures, synaptic activity in afferent inputs to striatum and activity of other intrastriatal neuronal elements.

In neocortex and hippocampus, FSI networks play a critical role in the organization and timing of gamma rhythms (e.g. Wang & Buzsaki, 1996; Klausberger *et al.*, 2003; Fries *et al.*, 2007; Cardin *et al.*, 2009). Striatal FSIs have a natural tendency to resonate at gamma frequencies (Bracci *et al.*, 2003; Taverna *et al.*, 2007) and, in response to current injection, they show burst firing with an average intraburst frequency of 52 Hz (Taverna *et al.*, 2007). They also possess dendritic gap junctions, which tend to result in enhanced, more broadly distributed gamma (Traub *et al.*, 2001). However, robust gamma rhythms in the brain typically involve active mutual feedback between excitatory and inhibitory neurons (for review see Whittington *et al.*, 2000) and excitatory neurons are not present in striatum. It thus appears most likely that fast striatal oscillations are paced externally rather than by intrastriatal mechanisms and this is consistent with the observed patterns of coherence with afferent structures. This does not exclude a major role for FSIs in transmitting fast oscillatory synchronization within striatum, especially as recent simulations indicate that gap junctions between FSIs lead to spike synchrony only when FSIs receive highly synchronous inputs (Hjorth *et al.*, 2009), as may occur during fast oscillations.

Do gamma oscillations contribute to striatal information processing?

The intrinsic properties of FSIs may have contributed to a particular sensitivity to fast rhythms in their inputs. FSIs have simpler, spineless dendrites and ionic currents that allow fast responses to excitatory inputs (e.g. Mallet *et al.*, 2005). In contrast, in ventral striatal MSNs the integration of afferent glutamatergic inputs into action potential generation appears to occur over a relatively broad, 40–60 ms time window (Wolf *et al.*, 2005; Moyer *et al.*, 2007), suggesting that they act more as pattern detectors than coincidence detectors. Fast oscillations are also found in corticostriatal neuron membrane

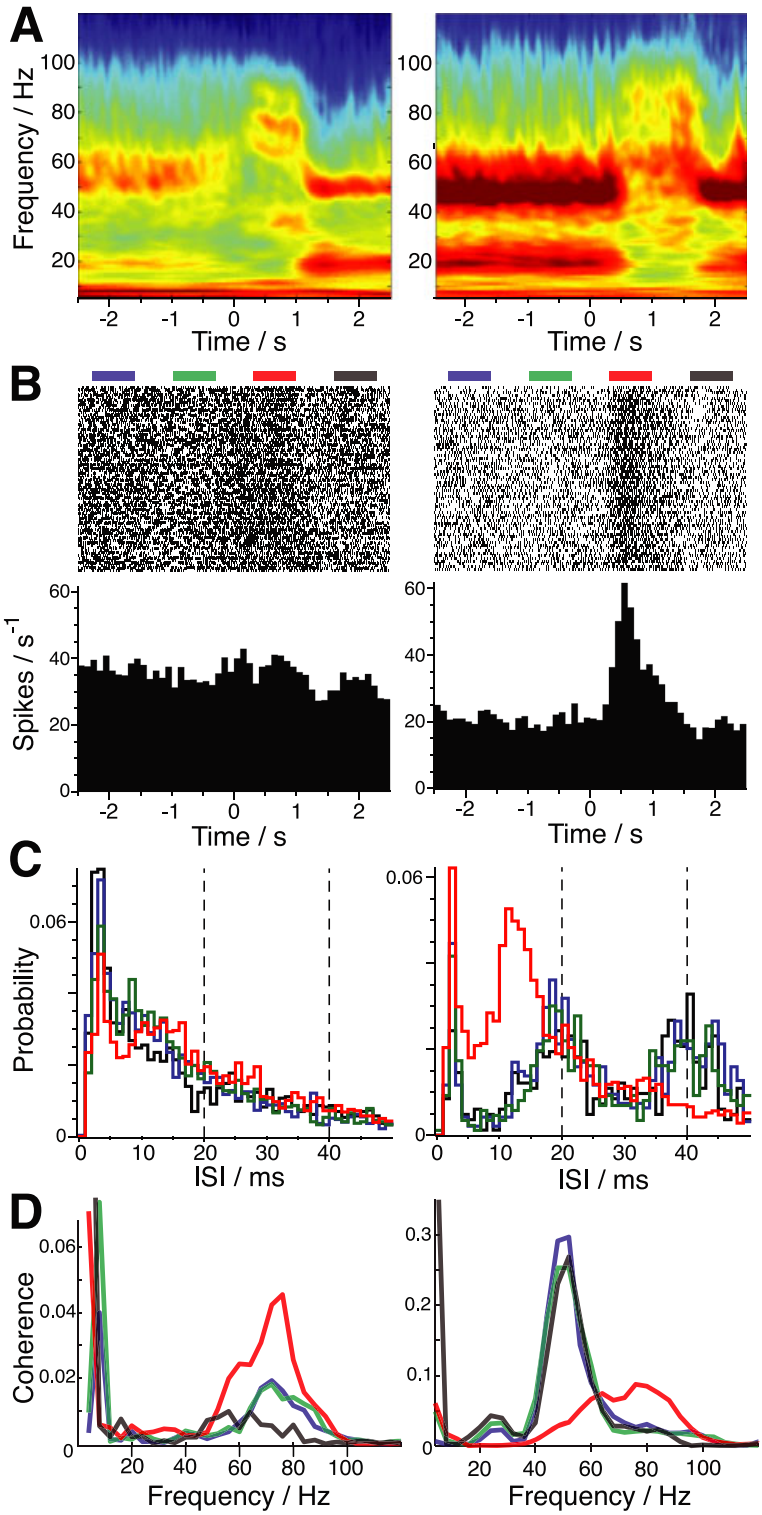

FIG. 5. Spike–LFP relationships during transient high-gamma epochs. Two examples (one in each column; from different rats) of joint LFP and single-neuron recordings during maze task performance. (A) Ventral striatal LFP oscillations surrounding arrival at reward ports; wavelet scalograms were calculated as in Fig. 4 but for rewarded trials only (n = 111 and 68 for the two examples). (B) Spike rasters and histograms for one neuron from each of the same tetrodes as the LFP recording used in A. Left neuron is a presumed striatal FSI (same neuron as Fig. 2, Aiii); right neuron had a complex double-peaked waveform and was unclassified. Note that the FSI on the left does not substantially change its firing rate during the increase in LFP high-gamma power. Colored bars above rasters indicate analysis periods used in C and D. (C) Histograms of inter-spike intervals (ISIs) (1 ms bins) for the two neurons in B. ISIs were calculated during four 0.7 s periods relative to arrivals at baited reward ports, and color coded (blue, −2.3 to −1.6 s; green, −1.0 to −0.3 s; red, + 0.3 to + 1.0 s; black, + 1.6 to + 2.3 s). The FSI on the left shows only subtle changes in the ISI distribution. The neuron on the right commonly fires at ∼20 or ∼40 ms intervals (corresponding to ∼50 Hz entrainment) but shows a dramatic, transient shift to shorter (∼2 and ∼12 ms) intervals, consistent with firing spike doublets at ∼80 Hz. (D) SFC plots. SFC is calculated during the same intervals as in C. Both neurons show a transient behavior-linked increase in high-gamma coherence to LFP.

potentials (Cowan & Wilson, 1994; Stern *et al.*, 1997) but not in MSN somatic membrane potentials (but see Kasanetz *et al.*, 2002), so the sluggish MSN response to input may tend to filter out fast oscillations in dendritic afferents.

However, given that FSIs are in a commanding position to synchronize striatal neurons into ensembles via rhythmic patterns of perisomatic $GABA_A$ input, why was only weak entrainment of MSNs to fast rhythms observed? There are probably several contributing factors, including technical limitations of this study. Firstly, entrainment is easier to detect with large numbers of spikes; whereas all of the FSIs were continuously active, most of our MSNs were silent for long periods of time and had low overall firing rates. However, for many MSNs thousands of spikes were recorded, which is sufficient for the detection of strong entrainment; in the same data set a substantial fraction of the same MSNs were found to be theta-entrained (Fig. 2A, iv) (Berke *et al.*, 2004, 2009). Secondly, most of our neurons were recorded in relatively dorsal parts of striatum, where fast rhythms tend to be weaker. Although this probably reduced the observed fraction of entrained cells, once again we had sufficient numbers of MSNs in relatively ventral and medial parts of striatum to see theta entrainment, which is rare in dorsal striatum (Berke *et al.*, 2004). Thirdly, to include as many spikes as possible in the analysis, cell entrainment was assessed using the whole session of behavioral task performance, using tools that assume a near-constant spike–LFP phase relationship. If individual MSNs show strong entrainment only at certain select moments during task performance, or vary their LFP phase (e.g. as different ensembles are 'selected'), this would have degraded the detection of entrainment. This possibility merits further investigation.

The FSI network was not acting as a unified, striatum-wide pacemaker for gamma oscillations; rather, the strong entrainment of individual FSIs appears to reflect the diversity of inputs driving this cell population (Berke, 2008). The distinct architecture of striatum seems to support more local information processing within largely segregated microcircuits compared with, e.g. hippocampus and piriform cortex whose longer range internal connectivity establishes a more integrated computational space (Buzsáki, 2006). The limited and variable striatal entrainment to fast oscillations is also consistent with the processing of specific types of input, rather than a general role in all striatal computation. In particular, the ∼50 Hz (and more transient ∼70 Hz) rhythms in rat striatum are probably directly related to olfactory and associated information. Although the piriform also appears to naturally resonate at ∼50 Hz (Neville & Haberly, 2004), piriform gamma oscillations are themselves driven by periodic inputs from the olfactory bulb and are interrupted if olfactory processing is prevented (e.g. by nasal occlusion; Vanderwolf, 2000).

It is conceivable that the high-gamma oscillations may have a more important general role given the very broad relationships between frontal cortex and striatum (reviewed in St-Cyr, 2003), and human studies have recently provided additional evidence for the relevance of such fast rhythms to the striatum. Ventral striatal LFP recordings from patients undergoing deep brain stimulator implants to treat depression have shown both mid-gamma (∼40 Hz) and high-gamma (∼70–100+ Hz) rhythms (Cohen *et al.*, 2009). These show power modulation during performance of a gambling task and are coupled to theta/alpha rhythms; such cross-frequency coupling has been observed in human neocortex (Canolty *et al.*, 2006), where it may facilitate the combination of local ensemble formation and long-range communication. Similar nesting of high-gamma rhythms within theta oscillations has recently been reported in rat striatum (Tort *et al.*, 2008), consistent with observations here of theta-nested high-gamma following amphetamine and joint entrainment of some striatal FSIs to both to theta and ∼80 Hz rhythms. By coordinating the entrainment of nearby striatal neurons to distinct oscillatory inputs, FSIs could make an important contribution to the overall functions of ventral striatum in 'gating' or 'switching' between different streams of afferent information. A deficit in striatal FSIs has been found in post-mortem tissue of human patients with Tourette syndrome (Kalanithi *et al.*, 2005), a condition featuring hard-to-suppress urges to perform actions, and a similar failure of FSI-mediated coordination within ventral striatal microcircuits might contribute to the failed suppression of thoughts in obsessive-compulsive disorder.

Of course human studies of basal ganglia LFP also suffer from uncertainty about LFP origins. Although strong striatal FSI entrainment makes it more reasonable to consider the potential significance of fast rhythms to striatal function, a conclusive demonstration of their functional role will probably require the use of new technologies (e.g. Cardin *et al.*, 2009) to directly manipulate these oscillations in behaving animals.

Dopamine and cortical-striatal oscillations in rats and humans

The observations here of a switch between different frequencies of striatal gamma rhythms demonstrate a novel manner in which specific events and psychoactive drugs can affect the physiology of cortical-basal ganglia circuits. They also suggest a specific role for dopamine in the control of these fast circuit dynamics and this is consistent with findings in human Parkinsonian patients of L-DOPA-induced switching from beta to high-gamma (70-85 Hz) oscillations elsewhere in the basal ganglia (e.g. Cassidy *et al.*, 2002). Striatal FSIs are a potentially relevant site of action of dopamine-induced frequency shifts, as at least *in vitro* they are depolarized by dopamine (Bracci *et al.*, 2002) and when depolarized have a higher frequency of intrinsic gamma-band membrane oscillations (Bracci *et al.*, 2003). However, several substantial limitations of the present study should provoke caution. Firstly, I used only systemic drug manipulations, so the relevant site of action may not be the striatum. Secondly, the gamma shift may not be the direct result of dopaminergic modulation on some pacemaking process but rather reflect an indirect action (e.g. on psychomotor arousal). Even if true, this possibility does not preclude an important impact of gamma changes on ongoing information processing, which contributes to the behavioral effects of stimulant drugs. Thirdly, although high-gamma power was greater on rewarded trials, arrival at both baited and unbaited reward ports prompted a switch in gamma frequencies. This is not what would be expected from a direct relationship to dopamine cell firing under the standard model (Schultz, 1998). However, dopamine measurements in this task have not been performed and recently both dopamine cell investigations (Matsumoto & Hikosaka, 2009) and striatal dopamine release measurements (Day *et al.*, 2007) have suggested an enhanced dopamine response to cues predicting either positive or negative outcomes. Interestingly, high-gamma oscillations in response to both positive and negative evaluations have recently been reported in LFPs recorded in the anterior cingulate cortex of monkeys (Quilodran *et al.*, 2008), and have been suggested to be important for learning from feedback. Cingulate and related cortical areas may thus be an important afferent source of high-gamma oscillations in striatum and the entrainment of single cells to these rhythms may contribute to reinforcement learning via spike-timing-dependent plasticity (Shen *et al.*, 2008), even if reward value is not the principal signal provided by increased high-gamma power.

Finally, I note that cortical-striatal circuits have an important role in time perception and that manipulations of dopamine neurotransmission can alter the apparent rate of time passage (reviewed in Lewis &

Miall, 2006; Meck *et al.*, 2008). Oscillatory activity has been proposed to be a critical underlying mechanism (Matell & Meck, 2004), so it is interesting that amphetamine can increase the frequency of cortical-striatal oscillations. Whether mediated via actions in striatum or in cortical structures such as prefrontal cortex, it would be remarkable if a stimulant-induced high-frequency 'buzz' turns out to be responsible for the subjective feeling of being 'buzzed'.

Supporting information

Additional supporting information may be found in the online version of this article:

Fig. S1. Frontal cortex maintains ~80–100 Hz coherence with striatum following amphetamine.

Please note: As a service to our authors and readers, this journal provides supporting information supplied by the authors. Such materials are peer-reviewed and may be re-organized for online delivery, but are not copy-edited or typeset by Wiley-Blackwell. Technical support issues arising from supporting information (other than missing files) should be addressed to the authors.

Acknowledgements

I thank Howard Eichenbaum for his mentoring and support, Lotus McDougal for technical assistance, Steven Kunec for contributions to the MATLAB code and Terry Robinson, Brandon Aragona, Greg Gage, Dan Leventhal and Anne West for critical reading of the manuscript. These results have previously appeared in shorter form (Berke *et al.*, 2003; Berke & Kunec, 2004; Berke, 2005). This work was funded by grants to J.D.B. from the National Institute on Drug Abuse, National Institute of Mental Health and Tourette Syndrome Association.

Abbreviations

ECoG, electrocorticogram; FSI, fast-spiking interneuron; LFP, local field potential; MSN, medium spiny projection neuron; SFC, spike-field coherence; STA, spike-triggered average.

References

Addison, P.S. (2002) *The Illustrated Wavelet Transform Handbook*. Institute of Physics Publishing, London.

Adrian, E.D. (1942) Olfactory reactions in the brain of the hedgehog. *J. Physiol.*, **100**, 459–473.

Albin, R.L., Young, A.B. & Penney, J.B. (1989) The functional anatomy of basal ganglia disorders. *Trends Neurosci.*, **12**, 366–375.

Berke, J.D. (2005) Participation of striatal neurons in large-scale oscillatory networks. In Bolamm, J.P., Ingham, C.A. & Magill, P.J. (Eds), *The Basal Ganglia VIII*. Springer, New York, pp. 25–35.

Berke, J.D. (2008) Uncoordinated firing rate changes of striatal fast-spiking interneurons during behavioral task performance. *J. Neurosci.*, **28**, 10075–10080.

Berke, J.D. & Kunec, S. (2004) Behavioral correlates of beta and gamma oscillations in the rat striatum. *Soc. Neurosci. Abstr.* 70.21.

Berke, J.D., Okatan, M., Skurski, J. & Eichenbaum, H.B. (2003) Synchronous striatal spindles and gamma-oscillations in freely-moving rats. *Soc. Neurosci. Abstr.* 390.16.

Berke, J.D., Okatan, M., Skurski, J. & Eichenbaum, H.B. (2004) Oscillatory entrainment of striatal neurons in freely moving rats. *Neuron*, **43**, 883–896.

Berke, J.D., Hetrick, V., Breck, J. & Greene, R.W. (2008) Transient 23–30Hz oscillations in mouse hippocampus during exploration of novel environments. *Hippocampus*, **18**, 519–529.

Berke, J.D., Breck, J.T. & Eichenbaum, H. (2009) Striatal versus hippocampal representations during win-stay maze performance. *J. Neurophysiol.*, **101**, 1575–1587.

Bevan, M.D., Magill, P.J., Terman, D., Bolam, J.P. & Wilson, C.J. (2002) Move to the rhythm: oscillations in the subthalamic nucleus-external globus pallidus network. *Trends Neurosci.*, **25**, 525–531.

Bracci, E., Centonze, D., Bernardi, G. & Calabresi, P. (2002) Dopamine excites fast-spiking interneurons in the striatum. *J. Neurophysiol.*, **87**, 2190–2194.

Bracci, E., Centonze D, Bernardi.G. & Calabresi, P. (2003) Voltage-dependent membrane potential oscillations of rat striatal fast-spiking interneurons. *J. Physiol.*, **549**, 121–130.

Buzsáki, G. (2002) Theta oscillations in the hippocampus. *Neuron*, **33**, 325–340.

Buzsáki, G. (2006) *Rhythms of the Brain*. Oxford University Press, New York.

Canolty, R.T., Edwards, E., Dalal, S.S., Soltani, M., Nagarajan, S.S., Kirsch, H.E., Berger, M.S., Barbaro, N.M. & Knight, R.T. (2006) High gamma power is phase-locked to theta oscillations in human neocortex. *Science*, **313**, 1626–1628.

Cardin, J.A., Carlén, M., Meletis, K., Knoblich, U., Zhang, F., Deisseroth, K., Tsai, L.H. & Moore, C.I. (2009) Driving fast-spiking cells induces gamma rhythm and controls sensory responses. *Nature*, **459**, 663–667.

Cassidy, M., Mazzone, P., Oliviero, A., Insola, A., Tonali, P., Di Lazzaro, V. & Brown, P. (2002) Movement-related changes in synchronization in the human basal ganglia. *Brain*, **125**, 1235–1246.

Cohen, M.X., Axmacher, N., Lenartz, D., Elger, C.E., Sturm, V. & Schlaepfer, T.E. (2009) Good Vibrations: Cross-frequency Coupling in the Human Nucleus Accumbens during Reward Processing. *J. Cogn. Neurosci.*, **21**, 875–889.

Cowan, R.L. & Wilson, C.J. (1994) Spontaneous firing patterns and axonal projections of single corticostriatal neurons in the rat medial agranular cortex. *J. Neurophysiol.*, **71**, 17–32.

Day, J.J., Roitman, M.F., Wightman, R.M. & Carelli, R.M. (2007) Associative learning mediates dynamic shifts in dopamine signaling in the nucleus accumbens. *Nat. Neurosci.*, **10**, 1020–1028.

Eeckman, F.H. & Freeman, W.J. (1990) Correlations between unit firing and EEG in the rat olfactory system. *Brain Res.*, **528**, 238–244.

Fogelson, N., Pogosyan, A., Kuhn, A.A., Kupsch, A., van Bruggen, G., Speelman, H., Tijssen, M., Quartarone, A., Insola, A., Mazzone, P., Di Lazzaro, V., Limousin, P. & Brown, P. (2005) Reciprocal interactions between oscillatory activities of different frequencies in the subthalamic region of patients with Parkinson's disease. *Eur. J. Neurosci.*, **22**, 257–266.

Fries, P., Reynolds, J.H., Rorie, A.E. & Desimone, R. (2001) Modulation of oscillatory neuronal synchronization by selective visual attention. *Science*, **291**, 1560–1563.

Fries, P., Nikolic, D. & Singer, W. (2007) The gamma cycle. *Trends Neurosci.*, **30**, 309–316.

Fukuda, T. (2009) Network architecture of gap junction-coupled neuronal linkage in the striatum. *J. Neurosci.*, **29**, 1235–1243.

Hammond, C., Bergman, H. & Brown, P. (2007) Pathological synchronization in Parkinson's disease: networks, models and treatments. *Trends Neurosci.*, **30**, 357–364.

Harris, K.D., Csicsvari, J., Hirase, H., Dragoi, G. & Buzsaki, G. (2003) Organization of cell assemblies in the hippocampus. *Nature*, **424**, 552–556.

Hjorth, J., Blackwell, K.T. & Kotaleski, J.H. (2009) Gap Junctions between Striatal Fast-Spiking Interneurons Regulate Spiking Activity and Synchronization as a Function of Cortical Activity. *J. Neurosci.*, **29**, 5276–5286.

Jones, M.W. & Wilson, M.A. (2005) Theta rhythms coordinate hippocampal-prefrontal interactions in a spatial memory task. *PLoS Biol.*, **3**, e402.

Kalanithi, P.S., Zheng, W., Kataoka, Y., DiFiglia, M., Grantz, H., Saper, C.B., Schwartz, M.L., Leckman, J.F. & Vaccarino, F.M. (2005) Altered parvalbumin-positive neuron distribution in basal ganglia of individuals with Tourette syndrome. *Proc. Natl Acad. Sci. USA*, **102**, 13307–13312.

Kasanetz, F., Riquelme, L.A. & Murer, M.G. (2002) Disruption of the two-state membrane potential of striatal neurones during cortical desynchronisation in anaesthetised rats. *J. Physiol.*, **543**, 577–589.

Kay, L.M. (2003) Two species of gamma oscillations in the olfactory bulb: dependence on behavioral state and synaptic interactions. *J. Integr. Neurosci.*, **2**, 31–44.

Kay, L.M., Beshel, J., Brea, J., Martin, C., Rojas-Libano, D. & Kopell, N. (2009) Olfactory oscillations: the what, how and what for. *Trends Neurosci.*, **32**, 207–214.

Klausberger, T., Magill, P.J., Marton, L.F., Roberts, J.D., Cobden, P.M., Buzsaki, G. & Somogyi, P. (2003) Brain-state- and cell-type-specific firing of hippocampal interneurons in vivo. *Nature*, **421**, 844–848.

Koos, T. & Tepper, J.M. (1999) Inhibitory control of neostriatal projection neurons by GABAergic interneurons. *Nat. Neurosci.*, **2**, 467–472.

Koos, T., Tepper, J.M. & Wilson, C.J. (2004) Comparison of IPSCs evoked by spiny and fast-spiking neurons in the neostriatum. *J. Neurosci.*, **24**, 7916–7922.

Kuhn, A.A., Kempf, F., Brucke, C., Gaynor Doyle, L., Martinez-Torres, I., Pogosyan, A., Trottenberg, T., Kupsch, A., Schneider, G.H., Hariz, M.I., Vandenberghe, W., Nuttin, B. & Brown, P. (2008) High-frequency stimulation of the subthalamic nucleus suppresses oscillatory beta activity in patients with Parkinson's disease in parallel with improvement in motor performance. *J. Neurosci.*, **28**, 6165–6173.

Laurent, G. (2002) Olfactory network dynamics and the coding of multidimensional signals. *Nat. Rev. Neurosci.*, **3**, 884–895.

Lewis, P.A. & Miall, R.C. (2006) Remembering the time: a continuous clock. *Trends. Cogn. Sci.*, **10**, 401–406.

Luk, K.C. & Sadikot, A.F. (2001) GABA promotes survival but not proliferation of parvalbumin–immunoreactive interneurons in rodent neostriatum: an in vivo study with stereology. *Neuroscience*, **104**, 93–103.

Magill, P.J., Bolam, J.P. & Bevan, M.D. (2000) Relationship of activity in the subthalamic nucleus-globus pallidus network to cortical electroencephalogram. *J. Neurosci.*, **20**, 820–833.

Mallet, N., Le Moine, C., Charpier, S. & Gonon, F. (2005) Feedforward inhibition of projection neurons by fast-spiking GABA interneurons in the rat striatum in vivo. *J. Neurosci.*, **25**, 3857–3869.

Matell, M.S. & Meck, W.H. (2004) Cortico-striatal circuits and interval timing: coincidence detection of oscillatory processes. *Brain Res. Cogn. Brain Res.*, **21**, 139–170.

Matsumoto, M. & Hikosaka, O. (2009) Two types of dopamine neuron distinctly convey positive and negative motivational signals. *Nature*, **459**, 837–841.

Meck, W.H., Penney, T.B. & Pouthas, V. (2008) Cortico-striatal representation of time in animals and humans. *Curr. Opin. Neurobiol.*, **18**, 145–152.

Mink, J.W. (1996) The basal ganglia: focused selection and inhibition of competing motor programs. *Prog. Neurobiol.*, **50**, 381–425.

Moyer, J.T., Wolf, J.A. & Finkel, L.H. (2007) Effects of dopaminergic modulation on the integrative properties of the ventral striatal medium spiny neuron. *J. Neurophysiol.*, **98**, 3731–3748.

Neville, K.R. & Haberly, L.B. (2004) Olfactory cortex. In Shepherd, G.M. (Ed) *The synaptic Organization of the Brain*. Oxford University Press, New York.

Nunez, P.L. & Srinivasan, R. (2006) *Electric Fields of the Brain*, 2nd Edn. Oxford University Press, Oxford.

Pare, D. & Gaudreau, H. (1996) Projection cells and interneurons of the lateral and basolateral amygdala: distinct firing patterns and differential relation to theta and delta rhythms in conscious cats. *J. Neurosci.*, **16**, 3334–3350.

Quilodran, R., Rothe, M. & Procyk, E. (2008) Behavioral shifts and action valuation in the anterior cingulate cortex. *Neuron*, **57**, 314–325.

Rojas-Libano, D. & Kay, L.M. (2008) Olfactory system gamma oscillations: the physiological dissection of a cognitive neural system. *Cogn. Neurodyn.*, **2**, 179–194.

Ruskin, D.N., Bergstrom, D.A., Kaneoke, Y., Patel, B.N., Twery, M.J. & Walters, J.R. (1999) Multisecond oscillations in firing rate in the basal ganglia: robust modulation by dopamine receptor activation and anesthesia. *J. Neurophysiol.*, **81**, 2046–2055.

Schultz, W. (1998) Predictive reward signal of dopamine neurons. *J. Neurophysiol.*, **80**, 1–27.

Shen, W., Flajolet, M., Greengard, P. & Surmeier, D.J. (2008) Dichotomous dopaminergic control of striatal synaptic plasticity. *Science*, **321**, 848–851.

Sirota, A., Montgomery, S., Fujisawa, S., Isomura, Y., Zugaro, M. & Buzsaki, G. (2008) Entrainment of neocortical neurons and gamma oscillations by the hippocampal theta rhythm. *Neuron*, **60**, 683–697.

St-Cyr, J.A. (2003) Frontal-striatal circuit functions: context, sequence and consequence. *J. Int. Neuropsychol. Soc.*, **9**, 103–128.

Stern, E.A., Kincaid, A.E. & Wilson, C.J. (1997) Spontaneous subthreshold membrane potential fluctuations and action potential variability of rat corticostriatal and striatal neurons in vivo. *J. Neurophysiol.*, **77**, 1697–1715.

Taverna, S., Canciani, B. & Pennartz, C.M. (2007) Membrane properties and synaptic connectivity of fast-spiking interneurons in rat ventral striatum. *Brain Res.*, **1152**, 49–56.

Tort, A.B., Kramer, M.A., Thorn, C., Gibson, D.J., Kubota, Y., Graybiel, A.M. & Kopell, N.J. (2008) Dynamic cross-frequency couplings of local field potential oscillations in rat striatum and hippocampus during performance of a T-maze task. *Proc. Natl Acad. Sci. USA*, **105**, 20517–20522.

Traub, R.D., Kopell, N., Bibbig, A., Buhl, E.H., LeBeau, F.E. & Whittington, M.A. (2001) Gap junctions between interneuron dendrites can enhance synchrony of gamma oscillations in distributed networks. *J. Neurosci.*, **21**, 9478–9486.

Tseng, K.Y., Kasanetz, F., Kargieman, L., Riquelme, L.A. & Murer, M.G. (2001) Cortical slow oscillatory activity is reflected in the membrane potential and spike trains of striatal neurons in rats with chronic nigrostriatal lesions. *J. Neurosci.*, **21**, 6430–6439.

Vanderwolf, C.H. (2000) What is the significance of gamma wave activity in the pyriform cortex? *Brain Res.*, **877**, 125–133.

Wang, X.J. & Buzsaki, G. (1996) Gamma oscillation by synaptic inhibition in a hippocampal interneuronal network model. *J. Neurosci.*, **16**, 6402–6413.

Whittington, M.A., Traub, R.D., Kopell, N., Ermentrout, B. & Buhl, E.H. (2000) Inhibition-based rhythms: experimental and mathematical observations on network dynamics. *Int. J. Psychophysiol.*, **38**, 315–336.

Wiltschko, A.B., Gage, G.J. & Berke, J.D. (2008) Wavelet filtering before spike detection preserves waveform shape and enhances single-unit discrimination. *J. Neurosci. Methods*, **173**, 34–40.

Wolf, J.A., Moyer, J.T., Lazarewicz, M.T., Contreras, D., Benoit-Marand, M., O'Donnell, P. & Finkel, L.H. (2005) NMDA/AMPA ratio impacts state transitions and entrainment to oscillations in a computational model of the nucleus accumbens medium spiny projection neuron. *J. Neurosci.*, **25**, 9080–9095.